



Contents lists available at ScienceDirect

Vision Research

journal homepage: www.elsevier.com/locate/visres

The joint effect of mesoscale and microscale roughness on perceived gloss

Lin Qi^{a,*}, Mike J. Chantler^b, J. Paul Siebert^c, Junyu Dong^a

^a Department of Computer Science, Ocean University of China, Qingdao, China

^b Texture Lab, Department of Computer Science, Heriot-Watt University, Edinburgh EH14 4AS, UK

^c School of Computing Science, University of Glasgow, Glasgow, UK

ARTICLE INFO

Article history:

Received 17 June 2014

Received in revised form 27 April 2015

Available online xxx

Keywords:

Rough surfaces

Perceived gloss

Mesoscale roughness

Microscale roughness

Conjoint measurement

ABSTRACT

Computer simulated stimuli can provide a flexible method for creating artificial scenes in the study of visual perception of material surface properties. Previous work based on this approach reported that the properties of surface *roughness* and *glossiness* are mutually interdependent and therefore, perception of one affects the perception of the other. In this case roughness was limited to a surface property termed *bumpiness*. This paper reports a study into how perceived gloss varies with two model parameters related to surface roughness in computer simulations: the mesoscale roughness parameter in a surface geometry model and the microscale roughness parameter in a surface reflectance model. We used a real-world environment map to provide complex illumination and a physically-based path tracer for rendering the stimuli. Eight observers took part in a 2AFC experiment, and the results were tested against conjoint measurement models. We found that although both of the above roughness parameters significantly affect perceived gloss, the additive model does not adequately describe their mutually interactive and nonlinear influence, which is at variance with previous findings. We investigated five image properties used to quantify specular highlights, and found that perceived gloss is well predicted using a linear model. Our findings provide computational support to the ‘statistical appearance models’ proposed recently for material perception.

© 2015 Elsevier Ltd. All rights reserved.

1. Introduction

Humans can recognise material properties from retinal images formed by the light reflected from objects in a scene. Researchers have proposed four classes of material attributes used by the vision system to characterise surface optical properties: *colour*, *gloss*, *translucency* and *texture* (Hutchings, 1999; Pointer, 2003).

Physical measurement of surface gloss usually requires instruments such as the *gloss meter* to record the intensity of reflected light at certain incident and reflected angles, whereas human visual perception of surface gloss has been found to be non-linearly related to instrument-based measurements under similar lighting conditions (Ji et al., 2006; Obein, Knoblauch, & Viénot, 2004).

Unlike the gloss meters that work under prescribed and constrained conditions, humans can perceive surface gloss in

numerous environments, even when the context is not known (Fleming, Dror, & Adelson, 2003). However, previous work has also revealed errors in human perception of gloss. Perceived gloss can vary with surface attributes that are physically distinct from the surface’s intrinsic specular reflectance, such as the surface geometry, illumination field, and viewing direction.

In computer graphics, surface reflectance is characterised by Bidirectional Reflectance Distribution Functions (BRDFs), and surface shape is characterised by a surface geometry model. Since each of these models describes the configuration of a surface at different spatial scales, and both relate to the attribute *roughness*. The focus of this paper is to investigate how surface roughness modulates perceived gloss as predicted by these models: we investigate how perceived gloss is influenced by microscale roughness from the BRDF model and mesoscale roughness from the surface geometry model. This classification of roughness is used by the authors for differentiating two roughness parameters in synthetic surface simulation using computer graphics. The remainder of this section will introduce these two types of roughness and review related previous work.

* Corresponding author.

E-mail addresses: qilin@ouc.edu.cn (L. Qi), M.J.Chantler@hw.ac.uk (M.J. Chantler), Paul.Siebert@glasgow.ac.uk (J.P. Siebert), dongjunyu@ouc.edu.cn (J. Dong).

1.1. Microscale roughness

The majority of studies in gloss perception use the analytical Bidirectional Reflectance Distribution Functions (BRDFs) to model surface optical properties when simulating material appearance in computer graphics, mainly due to the compact nature of these models (specified by only a few parameters) and their computational efficiency.

Light reflected from the surface, as illustrated schematically in Fig. 1(left), is described by most analytical BRDF models as a blended combination of a diffuse component and a specular component, where the blending proportions are controlled by two parameters (k_d and k_s). The specular component is characterised by the parameter α , used to specify the spread of the specular lobes, i.e. the rate of decay of the specularity as a function of angular viewing distance from the specular highlight centre.

In micro-facet theory, α parameterizes the roughness of the surface (Blinn, 1977; Kurt & Edwards, 2009; Torrance & Sparrow, 1967). The micro-facet model assumes that the surfaces are composed of many very tiny facets (micro-facets), where the normals of these micro-facets are distributed about the normal of an approximating local surface patch. The roughness (α) of the surface in microscale describes the degree to which micro-facet normals differ from the surface local normal. When the half-angle direction (i.e. the direction that bisects the lighting and the viewing directions) is close to the surface local normal, many of the micro-facets can be aligned in the half-angle direction to produce a bright specular highlight (Fig. 1(left) shows an example). When the half-angle direction is moving away from the surface local normal, fewer micro-facets can reflect light to the viewing direction, and therefore the intensity of the highlight falls-off. An illustration of the micro-facet surface and its imaging process is shown in Fig. 1(right).

This kind of roughness happens at the sub-pixel level, which means that it cannot be observed directly from the surface shape, but can only be perceived from the reflections from surfaces. We therefore name it *microscale roughness*, in contrast to the mesoscale roughness of the surface geometry model which will be introduced later.

In order to study the effect of variations in reflectance functions on perceived gloss, the use of spheres to define the reflecting surface under investigation has been widely reported (Ferwerda, Pellacini, & Greenberg, 2001; Fleming, Dror, & Adelson, 2001; Pellacini, Ferwerda, & Greenberg, 2000; Xiao & Brainard, 2008), since spherical geometry is simple to render and presents all

possible surface orientations to the viewer. The reported findings of these investigations all agree that perceived gloss shows a monotonic relationship with the microscale roughness parameter α , where rougher surfaces (in microscale) appear less glossy.

1.2. Mesoscale roughness

Surface geometry has been found to affect gloss perception significantly. Surface reflectance constancy is not guaranteed when the surface geometry is varied (Nishida & Shinya, 1998). When the explicit geometry of the surface is modelled at a lower resolution than the microscale roughness, we term the roughness that we can control through geometry as the *mesoscale roughness*.

The work reported in this paper is related to work carried out by Ho, Landy, and Maloney (2008) who studied how observers judge perceived bumpiness and glossiness using artificial 3D textures, and modelled the perceptual interactions of these two factors. Their experimental results show that increasing bumpiness increases perceived gloss, and that higher glossiness in turn increases perceived bumpiness.

Ho et al. (2008) employ an artificial surface model comprising specific (half ellipsoid) meso-structures which they manipulate by scaling their surface height (i.e. Root-Mean-Square surface height). However, it has been observed that surfaces exhibiting large RMS heights are unrealistic (Padilla, 2008), which naturally limits the range of roughness that can be investigated by means of this approach.

Ho et al. (2008) varied gloss levels by changing both the surface microscale roughness and the specular component parameters (α and k_s). In this work, we measure how perceived gloss is affected by variations in mesoscale and microscale roughness exclusively; hence we hold k_s constant.

The illumination configuration used by Ho et al. (2008) comprised an extended (area) light source positioned above and to the left of the observer. However, it has also been reported that such simple illumination schemes may limit the accuracy and reliability of observer percepts (Fleming et al., 2001, 2003).

Nevertheless, the conjoint measurement models are suggested by Ho et al. (2008) to be appropriate tools to study how perceived gloss is simultaneously affected by two or more properties. These models are employed in this paper and briefly described in the next subsection.

In our work we employ $1/f^\beta$ noise processes to model surfaces of a natural and isotropic appearance which have been found to resemble real-world surfaces (Mandelbrot, 1983; Voss, 1988).

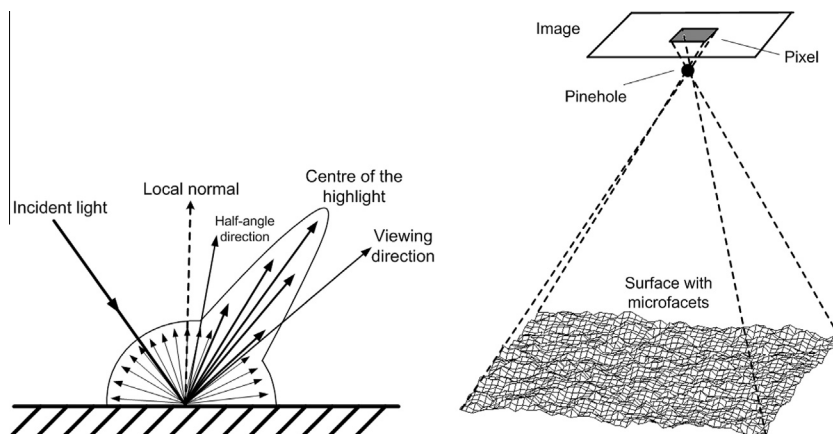


Fig. 1. Left: A schematic illustration of how light reflects from a surface with diffuse and specular reflections. Diffuse light is scattered in every direction of the hemisphere and the specular reflection is strongest in the mirror reflection direction (the centre of the highlight) and decays when it deviates from this direction. Right: A graphical illustration of micro-facets in the imaging process.

Furthermore, this approach requires only a few parameters which can be controlled easily. Padilla et al. reported that varying the roll-off term β of $1/f^\beta$ in the noise surface model affects perceived roughness significantly, therefore we investigate the role of β in perceived mesoscale roughness.

1.3. Additive model of perceived gloss and relief height

Ho et al. (2008) found that the relationship between relief height and perceived gloss can be described by an additive conjoint model. In the study presented here, we investigate how perceived microscale and mesoscale roughness varies in response to manipulating the parameters controlling surface reflectance and geometry. One of the main goals of our study is to test whether the joint effect of these two forms of roughness on perceived gloss is also linear and additive as reported in Ho et al. (2008).

The additive model assumes that microscale roughness α and mesoscale roughness β affect perceived gloss separately and additively. We employ the symbol G to denote the estimated gloss as below, and subscript 'ij' is used to denote the surface with microscale roughness level 'i' and mesoscale roughness level 'j'. The perceived gloss in the additive conjoint model G_{ij}^A is the sum of contributions from microscale roughness G^{α_i} and mesoscale roughness G^{β_j} for surface S_{ij} :

$$G_{ij}^A = G^{\alpha_i} + G^{\beta_j} = G_i^{\alpha} + G_j^{\beta} \quad (1)$$

We used the same decision model as Ho et al. (2008) to compare the results. The observers' paired comparison results for perceived gloss on surface S_{ij} and S_{kl} were assumed to comprise noise-contaminated decisions:

$$\Delta = G_{kl} - G_{ij}^* + \varepsilon, \quad \varepsilon \sim \text{Gaussian}(0, \sigma_g^2) \quad (2)$$

$\Delta > 0$ if surface S_{kl} is judged glossier than surface S_{ij} . ε represents the observer's precision in judgement, which we model using a Gaussian distribution of 0 mean and variance σ_g^2 .

1.4. Summary

Prior research has shown that both mesoscale and microscale roughness exhibit an affect on gloss perception, but their joint effect has not been well investigated. The purpose of this paper is to explore this joint effect using a geometric surface model on which $1/f^\beta$ noise is superimposed and a BRDF model, as described in detail in the following section.

2. Psychophysics experiment

The objective of the following psychophysics experiment is to investigate the joint effect of the meso and micro scale roughness parameters on perceived gloss. Our experimental design is based on presenting pairs of surfaces from the joint roughness space, described above, to observers who are then asked to indicate which surface from each pair appears to be more glossy.

2.1. Stimuli

The $1/f^\beta$ noise process was chosen to model the surface geometry used to generate height maps for reasons described in the introduction. To be self-contained, we shall introduce this model by reproducing the description we report in Qi et al. (2014), as follows:

Our height maps are generated to possess pseudo random phase spectra and magnitude spectra $H(f)$, scaled exponentially by roll-off factor β , as defined in Eq. (3):

$$H(f) = \frac{\sigma}{N(\beta)} f^{-\beta} \quad (3)$$

where β is the roll-off factor of the surface height magnitude spectrum or the inverse slope in log H -log f space; σ is the RMS (root mean squared) height of the surface. $N(\beta)$ is the normalising factor. This surface model is commonly termed as $1/f^\beta$, which derives from a simplification of Eq. (3). Note that the parameter β is inversely related to perceived roughness (Padilla et al., 2008). The magnitude spectra and phase spectra of the height maps comprised arrays of 512×512 pixels. Surfaces were generated for 5 levels of mesoscale roughness ($\beta = 1.6, 1.8, 2.0, 2.2, 2.4$). The RMS height was held constant at 17 pixels.

The Ashikhmin–Shirley gloss BRDF model (Ashikhmin & Shirley, 2000) was used to model the surfaces' optical properties¹ and the diffuse and specular component parameters of this model were fixed at $k_d = 0.4$, $k_s = 0.6$ respectively. The microscale roughness parameter α was logarithmically sampled for 5 levels ($\alpha = 0.02, 0.01, 0.005, 0.0025, 0.00125$). The microscale roughness levels used in producing the stimuli were chosen to be lower than that required to exhibit DOI (distinctness of image) gloss (Ferwerda et al., 2001; Pellacini et al., 2000).

An HDR (high dynamic range) environment map "StPeters" from Debevec's Light Probe Image Gallery (Debevec & Malik, 1997) was chosen as the lighting condition, as real-world illumination is complicated and its characteristics play an essential role in the perception of surface properties (Dror, Willsky, & Adelson, 2004).

We employed a physics-based path tracer, the "LuxRender" rendering system. Path tracing graphics can simulate a wide range of optical effects, the most important of these being more complex surface inter-reflections. The rendered images were linearly tone mapped to low dynamic range to match the display. The surfaces were displayed in the x-y plane (the viewing direction being parallel to the z-axis) and rotated cyclically in azimuth through an angular range of $w = \pm 12^\circ$ about the vertical (y) axis in 1° steps at 24 frames per second to generate an animated stimulus.

Since α and β parameterize microscale and mesoscale roughness respectively, we denote their levels instead of values for convenience. Thus surface S_{11} with parameter values α_1 and β_1 is the roughest stimulus in both scales, while the surface S_{55} is the smoothest in both scales. Fig. 2 shows the central image frames ($w = 0^\circ$) for each animated stimulus.

2.2. Apparatus

A 20-inch TFT LCD monitor (NEC LCD2090UXi) with a pixel pitch of 0.255 mm (100 dpi) was used to present the stimuli (resolution 1600×1200 pixels). A spectrophotometer (Gretag Macbeth Eye One Pro) was used to calibrate and linearise the gamma responses (1.0). The colour temperature was set to 6500 K. The maximum and minimum luminance was calibrated to 120 cd/m² and 0 cd/m². The monitor was set at a distance of 50 cm from the observer to provide an angular resolution of approximately 17 cpd. The stimuli subtended an angle of 14.89° in the vertical direction and the eyes of observer were approximately in line with the centre of the screen.

¹ We did not choose the Ward model that Ho et al. used in Ho et al. (2008) because we employed different rendering software. These two models are similar in terms of form and rendering quality (Ngan, Durand, & Matusik, 2005).

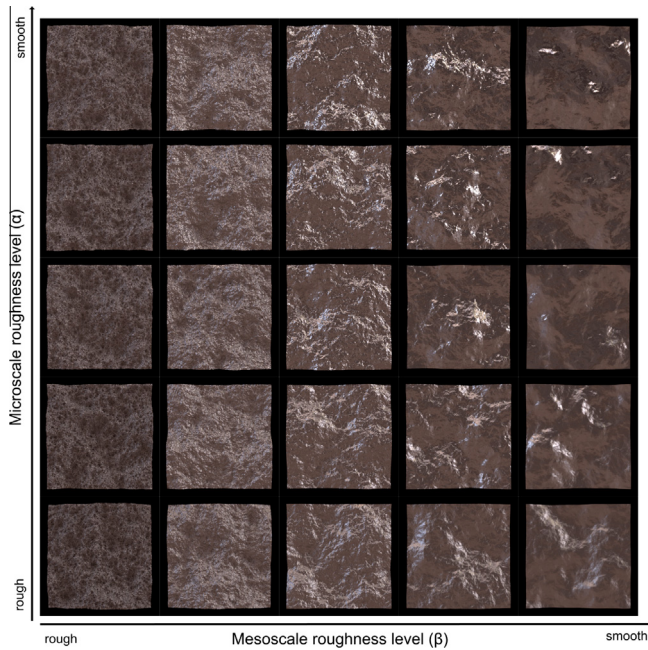


Fig. 2. Sample images of the stimuli. The central frame of each animated stimulus ($w = 0^\circ$) is shown. The x-axis denotes the mesoscale roughness level and the y-axis denotes the microscale roughness level. These images have been adjusted by a nonlinear gamma for display purposes.

2.3. Observers

Eight naïve observers with normal, or corrected-to-normal, vision participated in the experiment. All were students (or University employees) working in different fields, were less than 35 years of age, and of mixed gender and nationality. The experimental procedure was approved by the IRB (Institutional Review Board) of the university in accordance with The Code of Ethics of the World Medical Association (Declaration of Helsinki). The subjects signed informed consent and had the right to abandon the experiment at any time.

2.4. Procedure

All observers took part in a 2AFC (2 alternative forced choice) experiment. In each trial, a pair of stimuli was shown to the observer who was asked to choose the glossier stimulus of the pair. All combinations of the 25 stimuli (300 pairs) were shown in random order to each observer. To control the duration of the experiment, each animated stimulus was presented to the observer for a fixed period of time: in each trial, we randomly picked one stimulus from the pair and showed the animation once (rotating in sequence from 0° to -12° , then to 12° , and finally back to 0°). Following the presentation of a blank screen for 0.2 s, the second partner in the pair was displayed in the same way. The screen was then blanked until the observer indicated their decision as to which stimulus was glossier by pressing the corresponding keyboard key. Then the next pair was shown immediately. After completing the presentation of the 300 stimulus pairs, the procedure was then repeated another two times, which means that each pair was presented a total of three times in random order. All of the observers finished the experiment in between 60 and 75 min.

3. Results

3.1. Raw results

The 2AFC experimental results for all eight observers are presented in Fig. 3. Since this comparison matrix shows the raw experimental results it is not easy to observe patterns in these data. We therefore fitted the results using the conjoint measurement models, as detailed in the following section.

3.2. Fitting conjoint measurement models

The pair-wise comparison results from the experiment were used to fit the conjoint models for each observer by Maximum Likelihood Estimation (Ho et al., 2008; Knoblauch & Maloney, 2012). The resulting model parameters were normalised before averaging across observers.

We fitted the additive model and plotted the means of the model parameters from all eight observers in Fig. 4 with error bars showing the \pm standard error. This model separates observers'

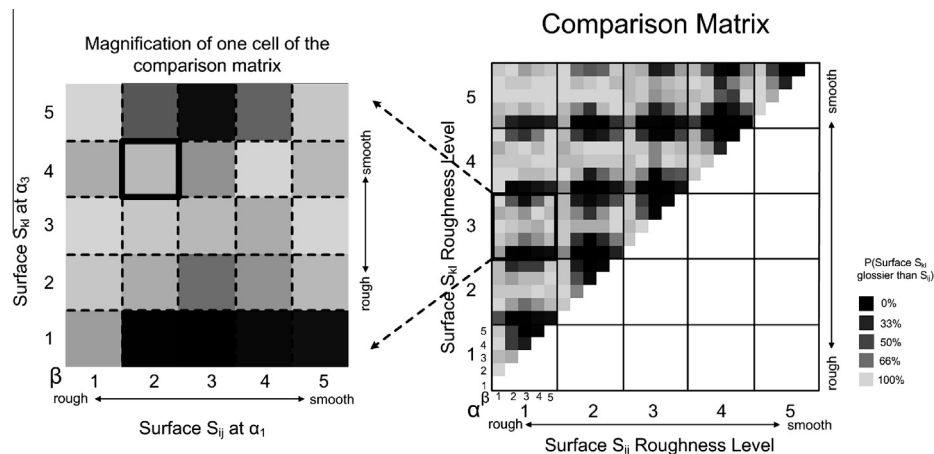


Fig. 3. Glossiness judgement results averaged across all 8 observers (the right matrix). The grey levels of the squares in the matrix represent the proportion of trials that a surface S_{kl} was perceived to be glossier than another surface S_{ij} , for each pair-wise comparison. Microscale roughness (α) level i (or k) is indicated by the large numeric labels (1, 2, ..., 5), and mesoscale roughness (β) level j (or l) is indicated by the small numeric labels (1, 2, ..., 5). The blocks in the solid grid represent different α levels, and block (1, 3), enclosed with bold boundaries, is shown magnified as an example (the left matrix). The grey level of the square enclosed with bold boundaries in the left matrix represents the proportion of time that surface S_{34} was perceived to be glossier than surface S_{12} .

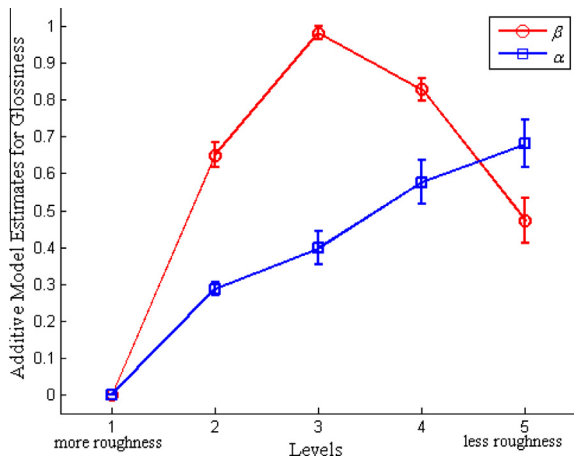


Fig. 4. Fitted parameters of the additive model. These are mean values averaged across the eight observers with the error bars denoting \pm standard errors. The two curves correspond to the parameters G_i^{β} ($i = 1 \dots 5$) and G_j^{α} ($j = 1 \dots 5$) respectively. The estimated gloss of a particular surface is the sum of the values from corresponding parameters.

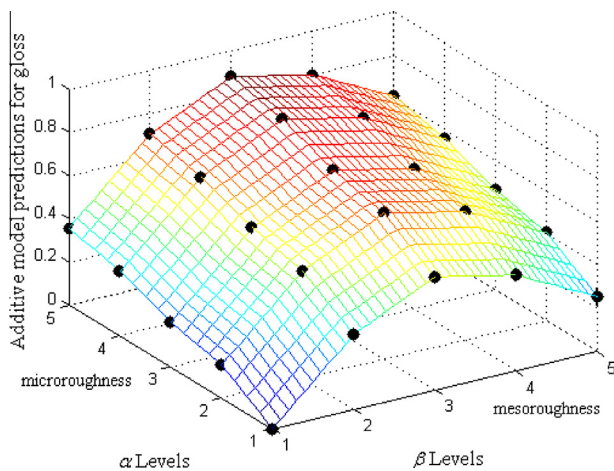


Fig. 5. Perceived gloss predicted by the additive model as a cojoint function of α and β .

judgement of surface glossiness into additive scales corresponding to mesoscale roughness and microscale roughness.

Fig. 5 shows the predictions of perceived gloss as a cojoint function of α and β using the additive model, scaled using the method suggested in Ho et al., 2008.

The perceived gloss for each surface (the ‘full model’ in Ho et al., 2008) was estimated in a similar manner to the additive model. Since the additive constraint was no longer present, the perceived gloss was estimated for each of the 25 surfaces (denoted as G_{ij}). The mean results across all observers are shown in Fig. 6 against β levels and α levels separately with error bars denoting the \pm standard error. The 3D plot of the predicted perceived gloss is shown in Fig. 7.

3.3. Comparing conjoint measurement models

To test whether both mesoscale roughness (β) and microscale roughness (α) have a statistically significant influence on perceived gloss, we compared the additive model with the two independent-property models using a nested hypothesis test as described in Ho et al. (2008). In the independent-property models,

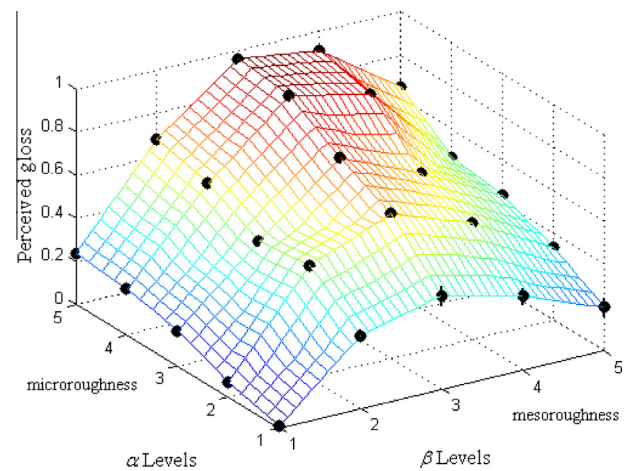


Fig. 7. 3D plot of predicted perceived gloss as a function of microscale roughness and mesoscale roughness using the model reported by Ho et al. (2008).

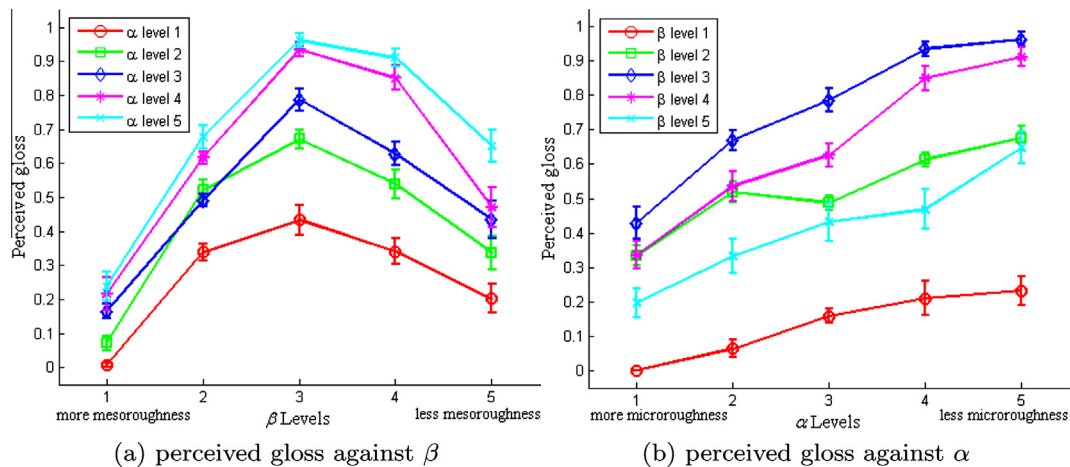


Fig. 6. Perceived gloss of each surface. These are mean values averaged across the eight observers with the error bars denoting \pm standard errors. The left graph plots perceived glossiness against β levels, where separate lines denote different α levels. The right graph plots perceived glossiness against α levels, where separate lines denote different β levels.

the task-irrelevant contributions (microscale roughness or mesoscale roughness) were fixed at zero. The likelihood-ratio was calculated and all eight observers' results revealed that the independent model was rejected using a Bonferroni-corrected significance test for $p < 0.001$. This suggests that both types of roughness significantly affect perceived gloss. This finding is consistent with that reported in Ho et al. (2008).

Ho et al. (2008) found that the additive model can adequately account for the interaction between bumpiness and glossiness, based on the results that 3 out of 6 observers showed significant results in a nested hypothesis test. However, this means that half of their results can not be accounted for by the additive model.

To test whether the additive model adequately accounts for our results, we compared the additive model with the perceived gloss in a nested hypothesis test. In contrast to Ho et al. (2008), we found that all eight observers' results were significant at a Bonferroni-corrected level of $p < 0.01$. Ho et al. (2008) conducted a linear regression on the predictions of the additive model against perceived gloss, and obtained high R^2 values for all observers. We also ran linear regressions for each observer's results to obtain R^2 values between 0.88 and 0.97. This suggests that although the additive model captures the variations in perceived gloss quite well, it is inadequate in describing the joint effect of mesoscale and microscale roughness on perceived gloss.

We can see that perceived gloss shows a monotonic relationship with α . This finding is consistent with literature (Ho et al., 2008; Fleming, Torralba, & Adelson, 2004; Pellacini et al., 2000). At each α level, the effect of mesoscale roughness, shows a non-monotonic (asymmetric bell-type curve) relationship with perceived gloss, which is consistent with our previous finding (Qi, Chantler, Siebert, & Dong, 2014). However, the test on conjoint measurement models differs from the findings of Ho et al. (2008) with regard to 'bumpiness'.

Fig. 8 shows the additive model predictions as dashed lines, and shows the perceived gloss predictions as solid lines. Note that the perceived gloss plots are copied from Fig. 6 and that the error bars have been removed for clarity. The differences between the additive model and the perceived gloss model predictions are shown in Fig. 9.

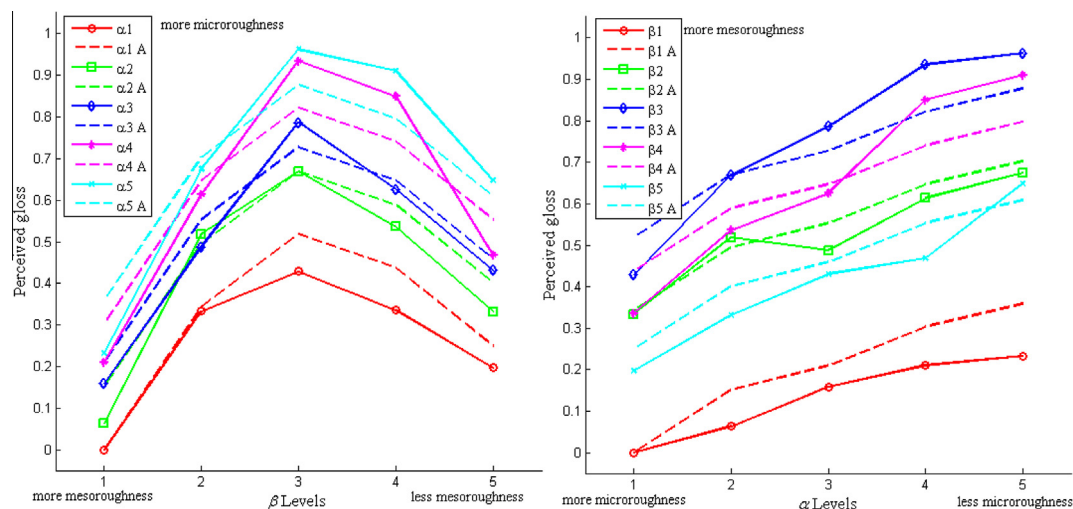


Fig. 8. Predictions of the additive model and the actual perceived gloss are shown together for comparison. The perceived gloss is plotted using solid lines while the additive model predictions are plotted using dashed lines. Left: Perceived gloss is plotted as a function of β level with separate curves denoting different α levels. Right: Perceived gloss is plotted as a function of α level with separate lines denoting different β levels. The legend in each plot denotes each curve, where the number next to α and β denotes the level and the letter 'A' denote the additive model.

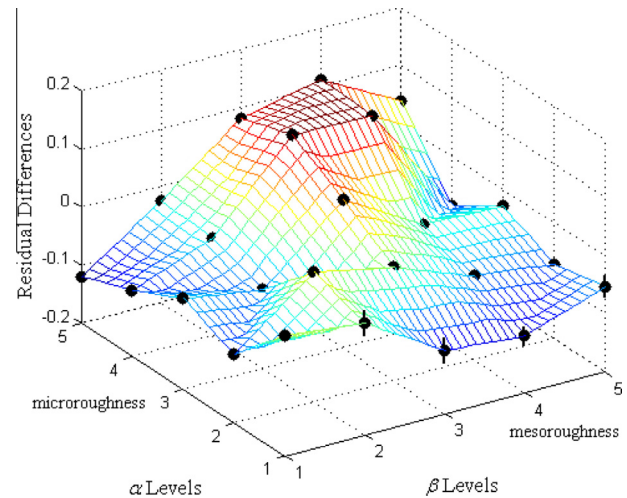


Fig. 9. A 3D scatter plot of the residual differences between the perceived gloss and the additive model predictions. The dots are record values averaged across all observers. The error bars show the \pm standard errors.

4. Discussion

Our experiments indicate that perceived gloss is modulated by model parameters of surface roughness in the mesoscale and microscale. However, in contrast with Ho et al. (2008), we observe that the joint effect of these two types of roughness on perceived gloss is not additive, but nonlinear.

Humans may use simple image statistics to infer surface gloss, such as the skewness of the luminance histogram (Motoyoshi et al., 2007). Although this finding has been challenged (Anderson & Kim, 2009), it suggests a hypothesis which considers more complex properties beyond first order image statistics. Marlow, Kim, and Anderson (2012) and our previous work (Qi et al., 2014) have reported that perceived gloss is well correlated with certain image properties of specular highlights. This suggests that the human vision system is likely to use surface appearance to estimate the magnitude of surface gloss (Fleming, 2014).

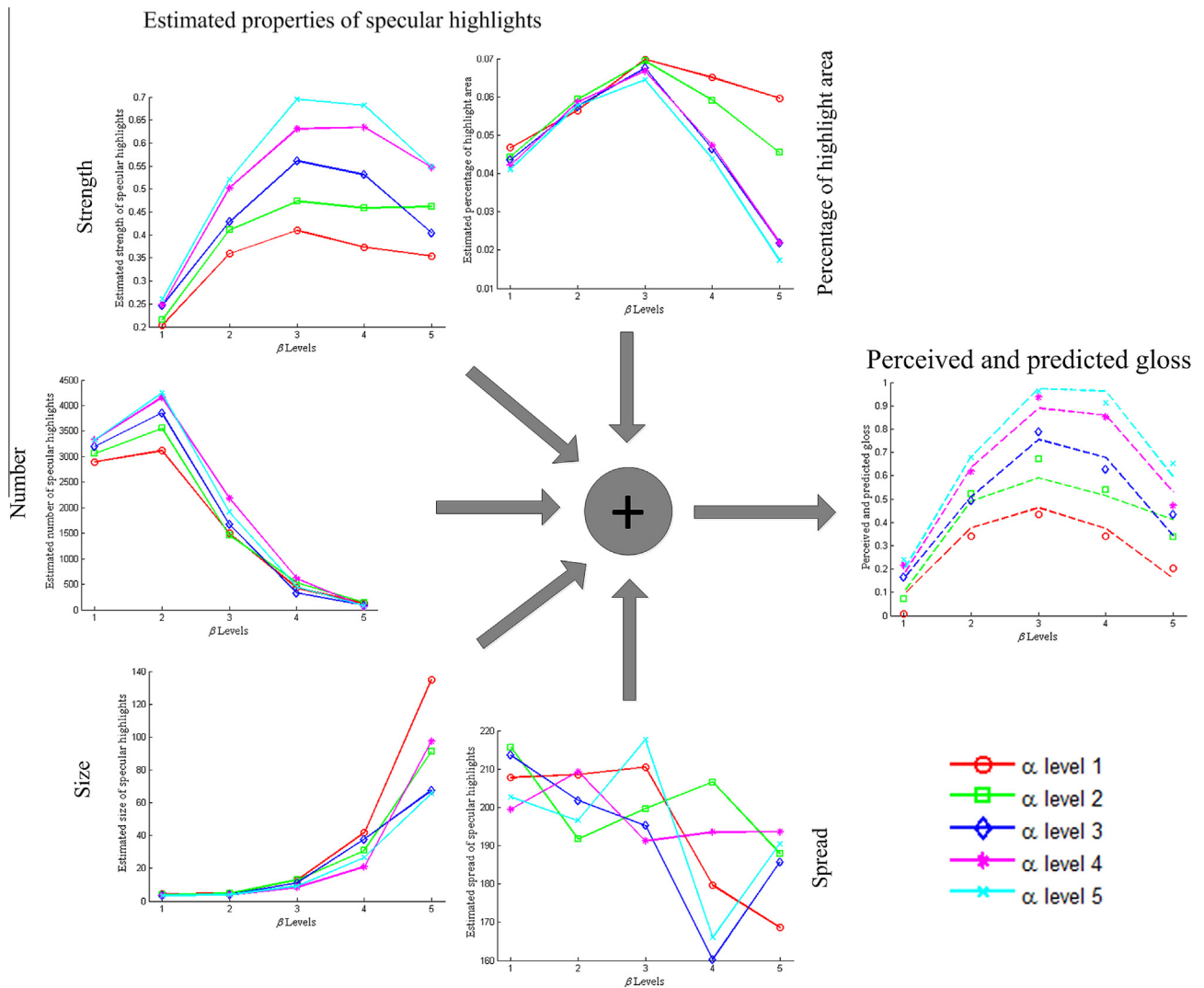


Fig. 10. Five estimated properties of specular highlights (percentage of highlight area, strength, number, size and spread) are plotted for each surface and presented in the graphs comprising solid lines. These estimated highlight properties were regressed with the perceived gloss of the full conjoint measurement model to produce the rightmost graph (comprising dashed lines) showing the regressed results.

Researchers have suggested several cues which observers might use to infer surface gloss and most previous work has concentrated on specular highlights and 'Distinctness Of Image gloss' (DOI gloss) (Beck & Prazdny, 1981; Blake & Bülthoff, 1990; Ferwerda et al., 2001; Kim, Marlow, & Anderson, 2011; Leloup et al., 2011; Marlow, Kim, & Anderson, 2011, 2012; Pellacini et al., 2000). In our experiments the microscale roughness parameters were specifically chosen so that DOI gloss was not obvious, and thus for our surfaces it is the specular highlights that are likely to provide the most important cues. Researchers have suggested a variety of attributes of specular highlights that affect observers' ratings: size, brightness (strength), contrast, sharpness, depth, orientation and placement (spread) (Beck & Prazdny, 1981; Berzhanskaya et al., 2005; Marlow et al., 2012). Marlow et al. (2012) employed psychophysics to measure specular highlight cues comprising contrast, sharpness, depth and coverage, and found a linear model that well predicts perceived gloss. Our own previous work found that the percentage of highlight area (equivalent to the coverage in Marlow et al.'s paper) accounts for most variations of perceived gloss (Qi et al., 2014).

Unfortunately, there is no commonly agreed method for segmenting specular highlights and most previous investigations have

undertaken manual analysis (Beck & Prazdny, 1981; Berzhanskaya et al., 2005; Kim et al., 2011; Marlow et al., 2011, 2012). In our previous work we used a simplistic image processing technique (Qi et al., 2014) which employed a simple definition of specular highlights based on a global intensity threshold. In this paper we use a similar method modified to incorporate an adaptive threshold. All pixels whose luminance values exceed two standard deviation above the global mean of the stimulus luminance are assumed to be specular highlight pixels. Adjacent highlight pixels are grouped together using an 8-nearest neighbourhood rule and each of the resulting 'connected components' are counted as a separate 'highlight areas'.

We calculate the number, strength, size, spread and percentage coverage of highlight areas for each of the 25 surfaces (i.e. they are calculated for each combination of α and β by averaging over the 25 images rendered from each surface). The number refers to the mean number of connected components, also averaged over the 25 images rendered from each surface. The strength of specular highlights refers to mean highlight pixel intensity. The number of pixels contained within each highlight is used to calculate the mean highlight size. The 2D centroid of each connected component is used both to represent the location of each highlight, and to

calculate their *spread* (spatial variation). The ratio of the total number of highlight pixels to the total number of surface pixels is used to derive the average (percentage) coverage of highlight areas.

We used multiple linear regressions to investigate the relationship between the five image statistics (introduced above) and perceived gloss. The results of this investigation are plotted in Fig. 10 with statistics $R^2 = 0.97$, $F(5, 19) = 119.99$, $p < 0.0001$, $MSE = 0.0533$.

Our regression results indicate that perceived gloss is highly related to the above listed image properties of specular highlights. This finding provides computational evidence that complements early studies (Beck & Prazdny, 1981; Blake & Bülthoff, 1990) and recent results reported by Marlow et al. (2012) and Marlow and Anderson (2013) who measured properties of specular highlights using psychophysical experiments and found these properties can linearly model perceived gloss.

5. Conclusions

In this paper, we investigated how perceived gloss is jointly affected by mesoscale roughness (β) and microscale roughness (α). Our work is related to that of Ho et al., 2008, who studied ‘bumpiness’ and glossiness.

Our findings are consistent with Ho et al. (2008) in that the microscale roughness exhibits a monotonic relationship with perceived gloss and the mesoscale roughness significantly affects perceived gloss. However, we have two novel findings that are at variance with Ho et al. (2008):

Firstly, the relationship between perceived gloss and mesoscale roughness is obviously non-monotonic for all microscale roughness levels used in the experiment. Ho et al. also noticed a slight decrease of gloss for their roughest, i.e. ‘bumpiest’, surfaces and reported this effect by commenting that: ‘the trend was less clearly monotonic’ Ho et al. (2008). They did not proceed to investigate ‘bumpier’ surfaces. We examined rougher surfaces and found that perceived gloss decreases for all α levels. This non-monotonicity is consistent with our previous findings Qi et al. (2014) and those reported by Marlow et al. (2012).

Secondly, we tested our experimental results against the conjoint measurement models as used by Ho et al. (2008). They found that the additive model is sufficient to describe the interaction between bumpiness and glossiness, whereas we found the additive model is rejected for all eight observers in our experiment. The difference between perceived gloss and that predicted by the additive model is due to the presence of the nonlinear component, which is manifest as the joint effect that the mesoscale and microscale roughness exert on perceived gloss. This observation was analyzed and explained by a hypothesis that perceived gloss is related to specular highlight cues which are modulated by the two types of surface roughness. Our hypothesis was tentatively tested by estimating the properties of specular highlights using simple image processing techniques.

In future investigations of gloss perception, it would be interesting to examine other properties of specular highlights which appear to be employed in human perception of gloss on rough surfaces, such as those tested by Marlow and Anderson (2013) using psychophysics methods. Furthermore, since microscale roughness can be tuned to produce DOI gloss cues on surfaces with low mesoscale roughness levels, the authors would like to compare this influence on perceived gloss with that of the gloss cues generated by specular highlights, as reported here.

Acknowledgment

This research is supported by China Postdoctoral Science Foundation (Grant No.: 2014M551963).

References

- Anderson, B. L., & Kim, J. (2009). Image statistics do not explain the perception of gloss and lightness. *Journal of Vision*, 9(11), 1–17. 10.
- Ashikhmin, M., & Shirley, P. (2000). An anisotropic phong brdf model. *Journal of Graphics Tools*, 5(2), 25–32.
- Beck, J., & Prazdny, S. (1981). Highlights and the perception of glossiness. *Attention, Perception, & Psychophysics*, 30, 407–410.
- Berzhanskaya, J., Swaminathan, G., Beck, J., & Mingolla, E. (2005). Remote effects of highlights on gloss perception. *Perception*, 34(5), 565–575.
- Blake, A., & Bülthoff, H. H. (1990). Does the brain know the physics of specular reflection? *Nature*, 343, 165–168.
- Blinn, J. F. (1977). Models of light reflection for computer synthesized pictures. *ACM SIGGRAPH Computer Graphics*, 11, 192–198.
- Debevec, P. E., & Malik, J. (1997). Recovering high dynamic range radiance maps from photographs. In *Proceedings of the 24th annual conference on Computer graphics and interactive techniques. SIGGRAPH '97* (pp. 369–378). New York, NY, USA: ACM Press/Addison-Wesley Publishing Co..
- Dror, R. O., Willsky, A. S., & Adelson, E. H. (2004). Statistical characterization of real-world illumination. *Journal of Vision*, 4(9 (Sep)), 821–837.
- Ferwerda, J. A., Pellacini, F., Greenberg, D. P. (2001). A psychophysically-based model of surface gloss perception. In *Proceedings SPIE Human Vision and Electronic Imaging*. pp. 291–301.
- Fleming, R. W. (2014). Visual perception of materials and their properties. *Vision Research*, 94, 62–75.
- Fleming, R. W., Dror, R. O., & Adelson, E. H. (2003). Real-world illumination and the perception of surface reflectance properties. *Journal of Vision*, 3(5), 347–368.
- Fleming, R. W., Torralba, A., & Adelson, E. H. (2004). Specular reflections and the perception of shape. *Journal of Vision*, 4(9), 798–820.
- Fleming, W., Dror, R. O., Adelson, E. H. (2001). How do humans determine reflectance properties under unknown illumination. In *Proceedings of CVPR workshop on identifying objects across variations in lighting: Psychophysics and computation*. pp. 347–368.
- Ho, Y., Landy, M., & Maloney, L. (2008). Conjoint measurement of gloss and surface texture. *Psychological Science*, 19(2), 196–204.
- Hutchings, J. (1999). *Food color and appearance. A Chapman & Hall food science book*. Aspen Publishers.
- Ji, W., Pointer, M. R., Luo, R. M., & Dakin, J. (2006). Gloss as an aspect of the measurement of appearance. *Journal of the Optical Society of America A*, 23(1), 22–33.
- Kim, J., Marlow, P., & Anderson, B. L. (2011). The perception of gloss depends on highlight congruence with surface shading. *Journal of Vision*, 11(9).
- Knoblauch, K., & Maloney, L. T. (2012). *Modeling Psychophysical Data in R*. New York: Springer-Verlag.
- Kurt, M., & Edwards, D. (2009). A survey of brdf models for computer graphics. *ACM SIGGRAPH Computer Graphics* 43, 4:1–4:7.
- Leloup, F. B., Pointer, M. R., Dutré, P., & Hanselaer, P. (2011). Luminance-based specular gloss characterization. *Journal of the Optical Society of America A*, 28(6), 1322–1330.
- Mandelbrot, B. B. (1983). *The fractal geometry of nature*. New York: W.H. Freedman and Co..
- Marlow, P., Kim, J., & Anderson, B. (2012). The perception and misperception of specular surface reflectance. *Current Biology*, 22(20), 1909–1913.
- Marlow, P., Kim, J., & Anderson, B. L. (2011). The role of brightness and orientation congruence in the perception of surface gloss. *Journal of Vision*, 11(9).
- Marlow, P. J., & Anderson, B. L. (2013). Generative constraints on image cues for perceived gloss. *Journal of Vision*, 13(14).
- Motoyoshi, I., Nishida, S., Sharan, L., & Adelson, E. (2007). Image statistics and the perception of surface qualities. *Nature*, 447(10), 206–209.
- Ngan, A., Durand, F., Matusik, W. (2005). Experimental analysis of brdf models. In *Proceedings of the eurographics symposium on rendering*. Eurographics Association, pp. 117–226.
- Nishida, S., & Shinya, M. (1998). Use of image-based information in judgments of surface-reflectance properties. *Journal of the Optical Society of America A*, 15(12), 2951–2965.
- Obein, G., Knoblauch, K., & Viénot, F. (2004). Difference scaling of gloss: Nonlinearity, binocularity, and constancy. *Journal of Vision*, 4(9).
- Padilla, S. (2008). Mathematical models for perceived roughness of three-dimensional surface textures. Ph.D. thesis, Heriot-Watt University.
- Padilla, S., Drbohlav, O., Green, P. R., Spence, A., & Chantler, M. J. (2008). Perceived roughness of $1/f^\beta$ noise surfaces. *Vision Research*, 48(17), 1791–1797.
- Pellacini, F., Ferwerda, J. A., & Greenberg, D. P. (2000). Toward a psychophysically-based light reflection model for image synthesis. In *SIGGRAPH '00: Proceedings of*

- the 27th annual conference on Computer graphics and interactive techniques (pp. 55–64). New York, NY, USA: ACM Press/Addison-Wesley Publishing Co..
- Pointer, M. R. (2003). Measuring visual appearance – a framework of the future. project 2.3 measurement of appearance. NPL Report COAM 19, November 2003, ISSN: 1475–6684, National Physical Laboratory, British Library Document Supply Centre, Boston Spa, Wetherby, West Yorkshire LS23 7BQ.
- Qi, L., Chantler, M. J., Siebert, J. P., & Dong, J. (2014). Why do rough surfaces appear glossy? *Journal of the Optical Society of America A*, 31(5 (May)), 935–943.
- Torrance, K., & Sparrow, E. (1967). Theory for off-specular reflection from roughened surfaces. *Journal of the Optical society of America*, 57(9), 1105–1114.
- Voss, R. F. (1988). Fractals in nature: From characterization to simulation. In H.-O. Peitgen & D. Saupe (Eds.), *The science of fractal images* (pp. 21–70). New York, NY, USA: Springer-Verlag New York Inc.
- Xiao, B., & Brainard, D. H. (2008). Surface gloss and color perception of 3D objects. *Visual Neuroscience*, 25, 371–385.